Proceedings World Geothermal Congress 2020+1
Reykjavik, Iceland, April - October 2021

Performance Study on U-tube Downhole Heat Exchanger Geothermal Systems with Various Working Fluids and Configurations

Chao Yu, Yiqun Zhang, Yawen Tan, Xianzhi Song, Haochen Huang, Yu Shi

China University of Petroleum (Beijing)

Keywords: geothermal energy, downhole heat exchanger, heat extraction performance, fluid parameters, heat exchanger configurations.

ABSTRACT

The downhole heat exchanger (DHE) geothermal system is suitable for exploitation of medium-low temperature geothermal resources, which has been widely used in space heating for residential and/or small-scale commercial buildings. The heat extraction performance of a U-tube DHE system with different working fluids remains unclear. In this paper, several 3D unsteady-state fluid flow and heat transfer models considering various configurations were established based on geological data of Shacheng geothermal field, China. Next, nine working fluids were selected and the datasets of real thermophysical parameters were established for each working fluid. Finally, a critical comparison of various working fluids for U-tube DHE systems with different configurations was carried out and the suitability of each working fluid under same condition was evaluated. This paper provides some different insights into medium-low temperature geothermal resources development and gives a good guidance for improving the heat extraction performance of DHE geothermal systems.

1. INTRODUCTION

Geothermal energy is a promising renewable energy resource with its advantages of low carbon emission, wide distribution and inexpensive price, which is an alternative choice to meet the increasing global energy demand (Fridleifsson, 2001; Song et al., 2017). It can provide a stable energy supply and it will not be influenced by weather and climate conditions just like some other renewable sources (Wang et al., 2020).

As for medium-low temperature geothermal resources, the most common development method is exploiting geothermal fluids; however, this may cause some problems, such as groundwater level decrease and ground subsidence (Song et al., 2018). Fortunately, a downhole heat exchanger (DHE) geothermal system, which extracts heat without exploiting any geothermal fluids from the reservoir, provides a better solution to us (Freeston and Pan, 1985; Lund, 2003). A typical schematic diagram of a single U-tube downhole heat exchanger geothermal system is shown in Figure 1. For a DHE system, the working fluid is injected into downhole heat exchanger through the inlet and then extracted from the outlet for direct/indirect use after a heat exchange process between the tube wall and working fluid. At the same time, the reservoir rock and geothermal fluid filled in borehole and reservoir keep providing heat to the pipe wall together. Besides, the flow of groundwater will also accelerate this heat exchange process.

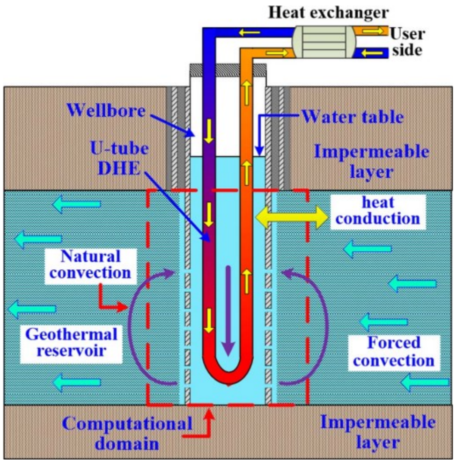

Figure 1: Schematic diagram of a single U-tube DHE system (Song et al., 2017)

A number of analytical and numerical models have been studied in order to analyze and evaluate the heat transfer performance of the DHE system. Carotenuto and Casarosa (2000) established a lumped parameters model to develop and extend to both single and double loop natural convection plant with the DHE, and found the limitations of the maximum heat transfer flow. And the model was successfully applied to evaluate the experimental data obtained in experimental tests. Tago et al. (2006) made a computer simulation program to study the heat extraction rate of a single U-tube downhole heat exchanger with square cross section, and checked the results with field experimental data of previous investigators. Results showed that the flow rate of the working fluid has a positive influence on the heat extraction performance. Luo et al. (2013) conducted a long-term experimental study of double U-tube DHE to compare the thermal performance of different borehole diameters. Results showed that thermal performance of larger diameter is better than smaller diameter. Shi et al. (2018) developed a transient state fluid flow and heat transfer DHE model with consideration of the natural convection, and studied the influence of some key parameters on heat production capacity, including reservoir porosity, permeability and thermal conductivity coefficient of rock. The above studies mainly focus on heat transfer process analysis and parameters optimization for single configuration of DHE, such as a single U-tube or double U-tube. Nevertheless, the configurations of heat exchanger also make great sense to heat extraction performance.

Previous researchers have done a lot of work to compare influence of various configurations. Zeng et al. (2003) developed a quasi-3D analytical model to describe the heat transfer process and temperature distribution along the length of DHE considering the axial heat flow of fluid. And the authors compared the performance of various configurations of DHE, such as single U-tube and double U-tube. Results showed that double U-tube is superior to single U-tube in terms of heat transfer performance. Jalaluddin et al. (2012) conducted a numerical and experimental study to analyze the performance of three types of DHE, including U-tube, double-tube and multi-tube, and found that the multi-tube DHE gives the best performance compared with the other two types and discontinuous operation can improve the heat transfer performance compared to the continuous operation. Bezyan et al. (2015) developed a 3D numerical model to investigate the heat transfer rate and temperature distribution of various heat exchangers and came to a conclusion that the spiral-shaped tube is the best configuration with the highest efficiency. Babak (2018) analyzed the thermal behavior of several different configurations of spiral heat exchangers using experimental and computational method and investigated the impacts of formation temperature and working fluid. There are few studies focusing on DHE system that borehole filled with thermal fluid. And the convective heat transfer mode surrounding a U-tube DHE is more complicated than the heat conduction in soil and grout (Dai et al., 2009). Thus, it's necessary to establish transient model to investigate heat extraction performance of various configurations of DHE considering heat convection of geothermal fluid.

In point of closed-loop geothermal system, the heat is brought to the surface for use without any direct contact between the working fluid and the geothermal reservoir. As a consequence, the working fluid has a significant impact on the heat transfer performance of closed-loop heat exchanger (Zhang et al., 2019). Previous researchers have done some jobs about performance of different working fluids in closed-loop system. For example, Davis and Michaelides (2009) established a numerical investigation to compare the production of isobutane with water from abandoned oil wells and found that isobutane has a better performance. Higgins et al. (2016) used SC-CO_2 as the working fluid rather than water in a U-shaped well and concluded that it can obtain more power compared to using water as working fluid. Conversely, Riahi et al. (2017) conducted a comparison between water and SC-CO_2 in closed-loop system and came to a conclusion that the power generation of water is in excess of that of SC-CO_2. However, there are few articles aiming at the evaluation and analysis about the heat extraction performance of various working fluids in DHE system, which also pertains to closed-loop geothermal systems.

In a summary, the previous researchers have done a lot of work and made great contribution to the development of U-tube DHE system. Nevertheless, studies on the performance of various working fluids in various U-tube DHE are lacking. The aim of this paper is to numerically analyze the transient heat transfer process and evaluate the heat extraction performance of U-tube DHE geothermal systems with various working fluids and configurations. This paper provides some different insights into medium-low temperature geothermal resources development and gives a good guidance for improving the heat extraction performance of DHE geothermal systems.

2. METHODOLOGY

2.1 Model assumptions

(1) The tubes and reservoir rock are regarded as homogeneous and isotropic, and their thermophysical properties are assumed to be constant and independent of temperature and pressure.
(2) The well was completed with open hole so that the wellbore was filled with geothermal fluids before the system running.
(3) The direction of groundwater flow is considered horizontal only.
(4) The fluid flow in DHE is simulated based on the assumption of a non-isothermal pipe flow.
(5) Formation temperature at side boundary remains constant and the top and bottom boundaries are regarded as impermeable.
(6) All the heat exchangers with different configurations have the same materials and wall thickness.
(7) To simplify the calculation, the working fluid in the wellbore is considered to be in the liquid state, and the phase transition is neglected.

2.2 Governing equations

For the geothermal reservoir, Darcy's Law and local thermal equilibrium between the rock and the fluid are employed to describe the fluid flow and heat transfer processes in reservoir, respectively. The governing equations are shown below:

$$v_g = -\frac{k}{\mu}\left(\nabla p + \rho_g g \nabla z\right) \tag{1}$$

$$\varphi \frac{\partial \rho_g}{\partial t} + \nabla \cdot \left(\rho_g v_g\right) = 0 \tag{2}$$

$$\left(\rho C_p\right)_{eff} \frac{\partial T_r}{\partial t} + \rho_g C_{pg} v_g \cdot \nabla T_r - \nabla \cdot \left(\lambda_{eff} \nabla T_r\right) = q \tag{3}$$

The Eq. (1) and Eq. (2) are the mass conservation equation and momentum equation, respectively. And the Eq. (3) is used to describe the local thermal equilibrium. The parameter q(W) is a heat source term. $(\rho C_p)_{eff}$ (J/(k·m^3)) and λ_{eff} (W/m·K) represent the effective volumetric heat capacity and effective thermal conductivity, respectively. They are calculated as follows:

$$\lambda_{eff} = (1-\varphi)\lambda_s + \varphi\lambda_g \tag{4}$$

$$(\rho C_p)_{eff} = (1-\varphi)\rho_s C_{ps} + \varphi\rho_g C_{pg} \tag{5}$$

The fluid flow in wellbore is described by the Navier-Stokes equation, of which the mathematical equations are as follows:

$$\varphi\frac{\partial\rho_g}{\partial t} + \nabla\cdot(\rho_g v_{gw}) = 0 \tag{6}$$

$$(\rho C_p)_{eff} = (1-\varphi)\rho_s C_{ps} + \varphi\rho_g C_{pg} \tag{7}$$

The wellbore is filled with geothermal fluid, which absorbs heat from the surrounding geothermal reservoir and then transfers the heat to working fluid via tube wall. This heat transfer process can be described as:

$$\rho_g C_{pg}\frac{\partial T_w}{\partial t} + \rho_g C_{pg} v_w \cdot \nabla T_w - \nabla\cdot(\lambda_g \nabla T_w) = -Q_{wall} \tag{8}$$

In this model, a non-isothermal pipe flow is employed to describe the fluid flow and heat transfer processes of the working fluid in the tube. The mathematical equations are as follows:

$$\rho_f\frac{\partial v_f}{\partial t} = -\nabla p - \frac{1}{2} f_D \frac{\rho_f}{D_p}|v_f| v_f \tag{9}$$

$$\frac{\partial(A_p\rho_f)}{\partial t} + \nabla_t\cdot(A_p\rho_f v_f) = 0 \tag{10}$$

$$\rho_f A_p C_{pf}\frac{\partial T_f}{\partial t} + \rho_f A_p C_{pf} v_f \cdot \nabla T_f = \nabla_t\cdot(A_p\lambda_f\nabla T_f) + \frac{1}{2} f_D \frac{\rho_f A_p}{D_p}|v_f| v_f^2 + Q_{wall} \tag{11}$$

Eq. (9) is a momentum equation and Eq. (10) is a mass conservation equation. f_D is the Darcy friction factor, which can be determined using the Churchill model (Churchill, 1977), as a function of the Reynolds number, determined by the roughness of the pipe surface and the pipe diameter. Eq. (11) is an energy conservation equation, and the second term on the right-hand side of the equation is the heat generated due to friction. The term Q_{wall} is the heat transferred by the geothermal fluid to the working fluid through the tube wall and it is equal to that in Eq. (8), which can be expressed as follows:

$$Q_{wall} = (hZ)_{eff}(T_{ext} - T_f) \tag{12}$$

The parameter $(hZ)_{eff}$ (W/(m·°C)) represents the total equivalent heat transfer coefficient. It is calculated using the following formula:

$$(hZ)_{eff} = \frac{2\pi}{\frac{1}{r_i h_{int}} + \frac{1}{r_o h_{ext}} + \frac{ln\left(r_o/r_i\right)}{\lambda_p}} \tag{13}$$

where h_{int} and h_{ext} (W/(m^2·°C)) represent the heat transfer coefficients of internal film and external film, respectively. They are determined as follows:

$$h_{int} = \frac{Nu_{int}\cdot\lambda}{D_p} \tag{24}$$

$$h_{out} = \frac{Nu_{out}\cdot\lambda}{D_p} \tag{35}$$

where Nu is the Nusselt number, representing a dimensionless temperature gradient near the pipe wall and the Nu_{int} can be calculated using the formula in ref. (Gnielinski, 1976):

$$Nu_{int} = \frac{\left(\frac{f_D}{8}\right)\times\left(Re\text{-}1000\right)\times Pr}{1+12.7\sqrt{\frac{f_D}{8}}\left(Pr^{\frac{2}{3}}\text{-}1\right)} \quad (16)$$

where *Re* and *Pr* represent the Reynolds and Prandtl numbers, respectively. And the Churchill and Chu correlation (Churchill and Chu,1975) was applied to calculate the Nu_{out}.

$$Nu_{out} = \left[0.6+\frac{0.387Ra^{1/6}}{\left(1+\left(0.559/Pr\right)^{9/16}\right)^{8/27}}\right]^2 \quad (17)$$

where the term *Ra* is Rayleigh number and the range of application is $Ra < 10^{12}$. The term T_{ext} (°C) in Eq. (12) can be determined by solving Eqs. (1) – (3), Eq. (6), and Eq. (7). Thus, the fluid flow and heat transfer in the geothermal reservoir, wellbore, and heat exchanger tube is coupled using the terms Q_{wall} and T_{ext}.

2.3 Initial and boundary conditions

In this paper, the geological data are taken from Shacheng geothermal field, China, where the Tianjin University has carried out a field trial (Dai et al., 2011). The reservoir was developed using a DHE together with a heat pump for space heating of vicinal dining hall. A U-tube DHE was installed in a test well with a depth of 117.5m, and a diameter of 280mm. The well has a permeable zone at about 55m to 100m from the surface according to the well temperature profile, which is shown in Figure 2. The maximum reservoir temperature is 62 °C and the averaged permeability of reservoir matrix is about 8.9×10^{-14} m^2, which was obtained from the well test data. The original subsurface water velocity in the reservoir is approximately 70 m/year. Thence, the length of the simulation model including U-tube DHE, reservoir and wellbore was set as 45m, which covered the whole permeable zone. The wellbore was filled with geothermal fluid and the temperature was set according to actual well temperature profile. The direction of groundwater flow is considered horizontal so that the top and bottom boundaries were considered as impermeable. The side boundary is in direct contact with the formation so that it was set as the same with initial reservoir temperature. In order to ensure that all working fluids are in liquid state, a proper pressure was given at inlet. The specific parameters for simulation cases are listed in Table 1.

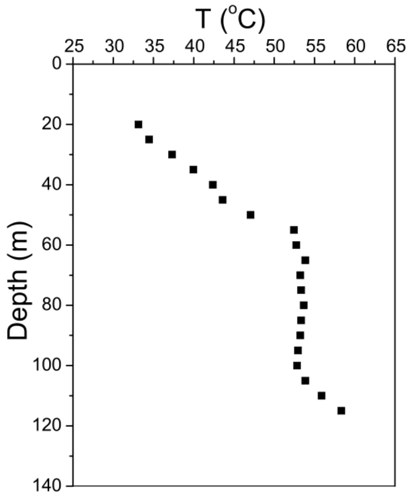

Figure 2: Well temperature profile (Dai et al., 2011)

Table 1: Default parameters for simulation cases

Items	Values
Diameter of wellbore (m)	0.28
Diameter of formation (m)	5
Total length of well (m)	45
Porosity of permeable zone	0.35
Permeability of permeable zone (mD)	2000
Porosity of reservoir matrix	0.1
Permeability of reservoir matrix (mD)	89
Inlet temperature of working fluid (°C)	20
Inlet volume flow of working fluid (m^3/h)	0.4
Formation thermal conductivity (W/(m·°C))	3
Rock specific heat capacity (J/(m·°C))	860

Rock density (kg/m^3)	2650
Original subsurface water velocity (m/year)	70

2.4 Finite-element method

The finite element solver COMSOL is utilized to solve the partial differential equations (PDEs) of the established three-dimensional unsteady-state numerical model. As for the proposed model, the heat transfer and thermal fluid flow in the wellbore and the surrounding reservoir are simulated using a three-dimensional model. Regarding the DHE, the fluid flow and heat transfer processes of the tubes are described using a non-isothermal pipe flow model, in which the tubes are represented by one-dimensional lines. As for the simulation mesh scheme, the swept mesh method is employed, which is shown in Figure 3. The triangular elements are first generated on the top surface, and then they are swept along the axial direction to the opposite bottom surface to produce triangular prism elements. It is noted that the meshes near the top, bottom, and wellbore boundaries are refined to avoid boundary effects. In this paper, four configurations of DHE are investigated, including single U-tube, serial double U-tube, parallel double U-tube, and spiral tube. The four types DHE tubes that represented by one-dimensional lines are meshed by the edges mesh node. This method can reduce the computational time and ensure computational accuracy.

The spiral tube DHE is the most complicated among the selected four, so that it is used to prove the irrelevance between mesh number and simulation results. The outlet temperature after half an hour of the spiral tube DHE with different mesh numbers are calculated and the results are shown in Figure 4. It indicates that the computational time increases dramatically with the increase of mesh number. When the mesh number is more than 40000, the outlet temperature remains unchanged. However, when the mesh number is less than 26000, the simulation results are completely different. Therefore, considering the computational time and accuracy of results, it is reasonable to perform the simulation with a mesh number of 40000 in the following analysis.

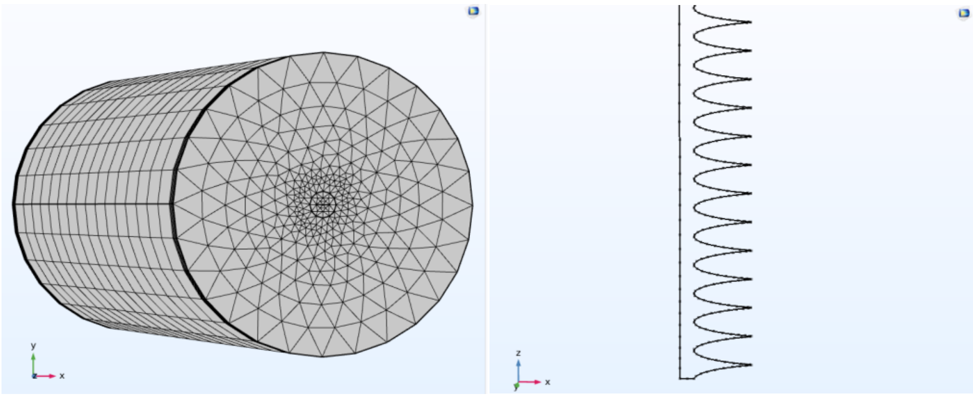

(a) Meshing schemes of whole model **(b) Meshing schemes of spiral tube**

Figure 3: The numerical meshing schemes

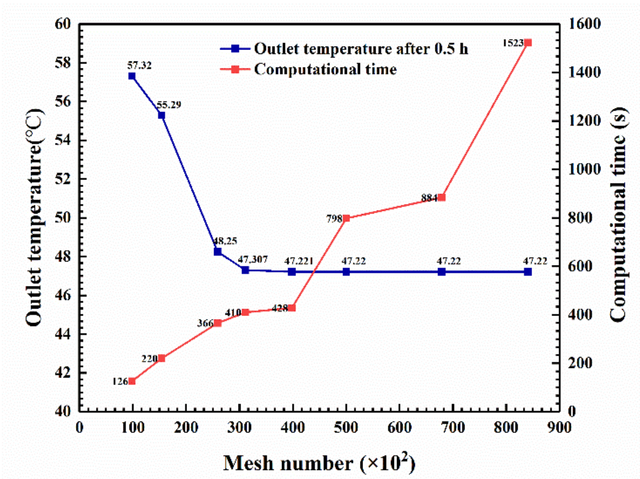

Figure 4: The outlet temperature and computational time under various mesh numbers

3. COMPARISON AND DISCUSSION

The thermal power is introduced to describe the heat extraction performance and is defined as follows:

$$P_{out} = 0.001 \times \left(Q_{out} C_{pf,out} T_{f,out} - Q_{in} C_{pf,in} T_{f,in} \right) \tag{18}$$

where Q_{in} (kg/s) and Q_{out} (kg/s) represent inlet mass flow rate and outlet mass flow rate of working fluids, respectively.

In this study, nine safe and environmentally friendly working fluids are selected for investigation considering their chemical stability and cost, which includes water, CO_2, R134a, R152a, R227ea, R245fa, R1234ze, R600a, and pentane. Based on the NIST Reference Fluid Thermodynamic and Transport Properties software (REFPROP), real thermophysical parameters datasets, including the density, thermal capacity at constant pressure, viscosity, thermal conductivity, and specific heat ratio, are established. The real thermophysical parameter datasets considering the variations in the parameters with pressure and temperature are applied to the cases, which includes three configurations of DHE, such as single U-tube, double U-tube, and spiral tube. In the simulation cases, the inlet temperature and volume flow are set to 20 °C and 0.4 m^3/h, and the other wellbore and reservoir parameters are based on the field data, which have been introduced in Section 2.3. And the production time in the simulation model is set to 12 h.

3.1 Single U-tube

This sub-section presents a comparison of the heat extraction performance of nine different circulating fluids in a single U-tube. The outlet temperature and thermal power of the nine working fluids are shown in Figure 5 and the circulation pressure loss is shown in Figure 6.

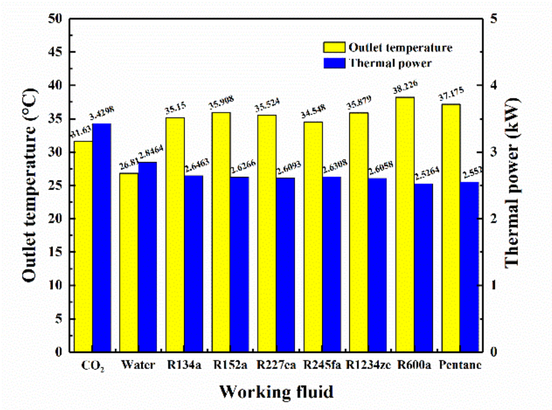

Figure 5: Outlet temperature and thermal power of different working fluids for single U-tube

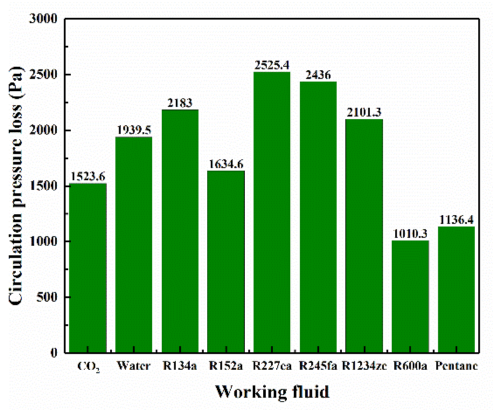

Figure 6: Circulation pressure loss of different working fluids for single U-tube

As can be seen from Figure 5, the outlet temperature corresponding to the selected seven organic working fluids and CO_2 are basically higher than water, indicating that the convective heat transfer coefficients of these organic working fluids are relatively high and most of them are better than water. This can be explained as the difference in heat flux for convective heat transfer between the different working fluids and the reservoir under the same working conditions is small, and the specific heat capacity of the organic working fluids is much smaller than that of water, so the outlet temperature will be higher when they extract a similar amount of heat. However, the thermal power of the organic working fluids is lower than that of water and much lower than that of CO_2. The thermal power of CO_2 is about 20% higher than that of water and about 30% higher than that of R134a, which is the most powerful organic working fluids. As can be seen from Figure 6, R600a and pentane have the lowest pressure loss, but they also have the lowest thermal power, while the pressure loss of CO_2 is only higher than these two. Taking into account the thermal power, outlet temperature and pressure loss, it can be concluded that CO_2 is the optimum heat extraction working fluid.

3.2 Double U-tube

In this sub-section, the single U-tube is replaced by a double U-tube and the other parameters are the same as in the previous sub-section. the outlet temperature and thermal power for the nine circulating fluids are shown in Figure 7 and the circulation pressure loss is shown in Figure 8.

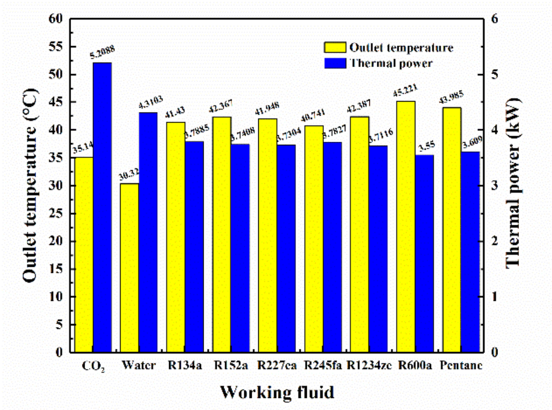

Figure 7: Outlet temperature and thermal power of different working fluids for double U-tube

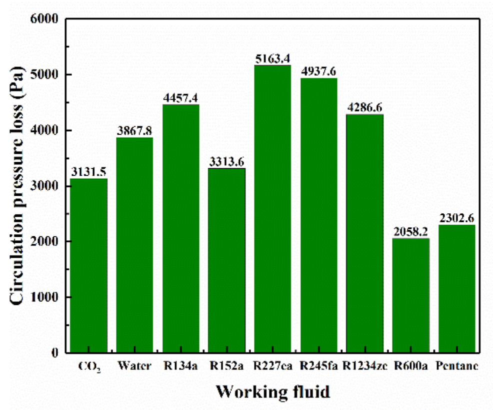

Figure 8: Circulation pressure loss of different working fluids for double U-tube

As can be seen from Figure7, the outlet temperature corresponding to the selected seven organic working fluids and CO_2 are basically higher than that of water, but the thermal power of the organic working fluids are all lower than water and much lower than CO_2, which is the same conclusion reached using the single U-tube. The thermal power of CO_2 is about 21% higher than that of water and about 37% higher than that of R134a, the most powerful organic working fluids. The advantage of CO_2 over both becomes greater. As can be seen in Figure 8, R600a and pentane have the lowest cycle pressure loss, but they also have the lowest thermal power, while CO_2 only has a higher cycle pressure loss than these two. Taking into account the thermal power, outlet temperature and pressure loss, it can be concluded that CO_2 is the optimum working fluid and has more advantages.

3.3 Spiral tube

In this sub-section, the double U-tube is replaced by a spiral tube and the other parameters are the same as in the previous sub-section. The outlet temperature and thermal power for the nine circulating fluids are shown in Figure 9 and the circulation pressure loss is shown in Figure 10.

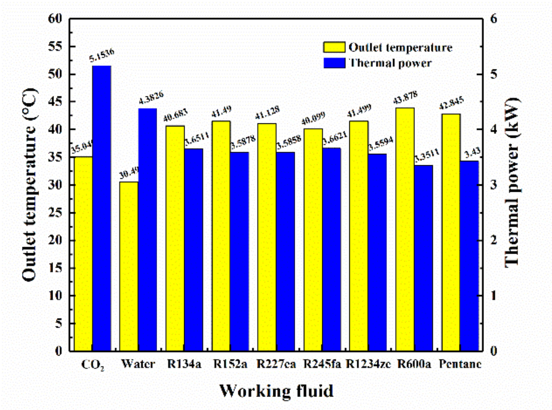

Figure 9: Outlet temperature and thermal power of different working fluids for spiral tube

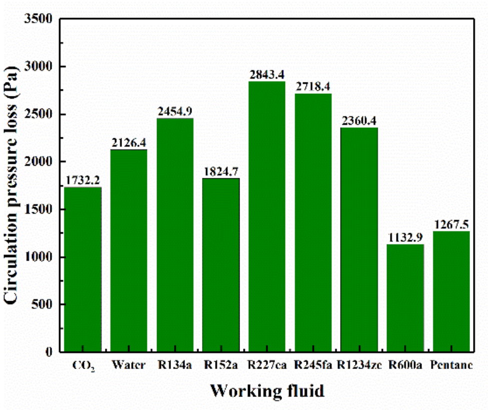

Figure 10: Circulation pressure loss of different working fluids for spiral tube

As can be seen from Figure 9, the outlet temperatures corresponding to the seven selected organic working fluids and CO_2 are basically higher than that of water, while the thermal power of the organic working fluids is lower than that of water and much lower than that of CO_2. The thermal power of CO_2 is about 18% higher than that of water and about 41% higher than that of the highest organic working fluids, R134a, giving CO_2 a greater advantage over the organic process but a smaller advantage over water. As can be seen from Figure 10, R600a and pentane have the lowest pressure loss, but they also have the lowest thermal power, while the pressure loss of CO_2 is only higher than these two. Taking into account the thermal power, outlet temperature and pressure loss, it can be concluded that CO_2 is the optimum working fluid. Under such conditions and evaluation criteria, water has a greater advantage over organic fluids and can also be considered as the superior working fluid.

3.4 Discussion of three configurations

As shown above, the comparison results of various working fluids for U-tube DHE systems with different configurations are similar. Among the nine working fluids, CO_2 exhibits the highest thermal power, followed by water. R600a and pentane have the lowest pressure loss, but they also have the lowest thermal power. As for U-tube DHE systems, thermal power is the most important index of heat extraction performance. We can come a conclusion that CO_2 is the optimum working fluid, which is followed by water. Therefore, we use CO_2 and water as examples for further analysis of three configurations. The outlet temperature and thermal power for the three configurations are shown in Figure 11 and the circulation pressure loss is shown in Figure 12.

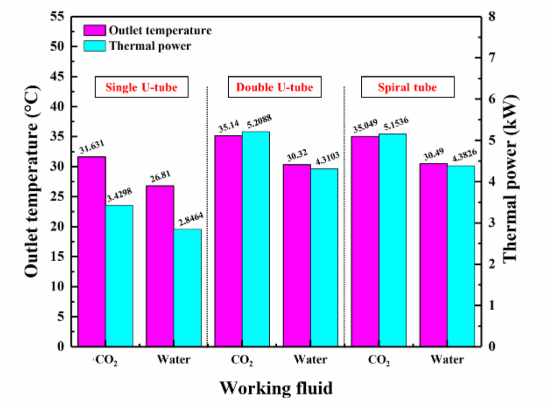

Figure 11: Outlet temperature and thermal power of three configurations

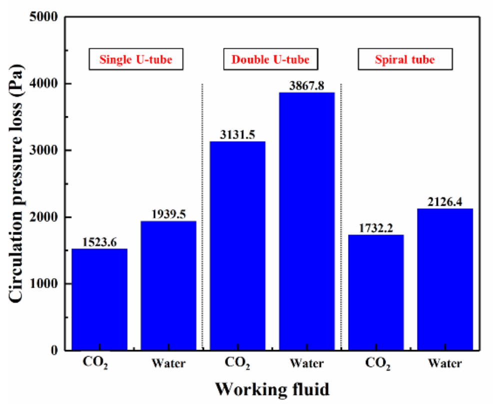

Figure 12: Circulation pressure loss of different working fluids three configurations

It is shown in Figure 11 that the heat extraction performance of three types of DHE structures are different with various working fluids. When using CO_2 as working fluids, the double U- tube DHE performs the best. And when using water as working fluid, the spiral tube DHE performs the best. Thus, the choice of configurations and working fluids should be made according to realistic situations.

4. CONCLUSION

In this paper, several 3D unsteady-state fluid flow and heat transfer models considering various configurations were established based on geological data of field trial. And a critical comparison of various working fluids for U-tube DHE systems with different configurations was carried out and the suitability of each working fluid under same condition was evaluated. The main conclusions of this study are drawn as follows:

(1) The comparison results of various working fluids for U-tube DHE systems with different configurations are similar. Among the nine working fluids, CO_2 exhibits the highest thermal power, followed by water. R600a and pentane have the lowest pressure loss, but they also have the lowest thermal power.

(2) As for U-tube DHE systems, thermal power is the factor which can best characterize the heat extraction performance. It can be concluded that CO_2 is the optimum working fluid. Under such conditions and evaluation criteria, water has a greater advantage over organic fluids and can also be considered as the superior working fluid.

(3) Among the three types of DHE structures, single U-tube, double U- tube and spiral tube, the double U- tube performs the best for heat extraction when using CO_2 as working fluid and spiral tube performs the best when using water as working fluid. The choice of configurations and working fluids should be made according to realistic situations.

(4) This paper provides some different insights into medium-low temperature geothermal resources development and gives a good guidance for improving the heat extraction performance of DHE geothermal systems. However, influences of key parameters on DHE heat extraction performance have not been examined, which is part of following work.

ACKNOWLEDGEMENT

This study was funded by the National Key Research and Development Program of China (Grant No. 2018YFC0604304) and National Natural Science Funds for Excellent Young Scholars of China (Grant No. 51822406).

REFERENCES

Babak, D.B.: Effectiveness of using spiral ground heat exchangers in ground source heat pump system of a building for district heating/cooling purposes: Comparison among different configurations, *Applied Thermal Engineering*, **130**, (2018), 1489-1506.

Bezyan, B., Porkhial, S., and Mehrizi, A.A.: 3-D simulation of heat transfer rate in geothermal pile-foundation heat exchangers with spiral pipe configuration, *Applied Thermal Engineering*, **87**, (2015), 655-668.

Carotenuto, A., and Casarosa, C.: A lumped parameter model of the operating limits of one-well geothermal plant with down hole heat exchangers, *International Journal of Heat and Mass Transfer*, **43**, (2000), 2931-2948.

Churchill, S.W.: Friction factor equation spans all fluid-flow regimes, *Chemical Engineering*, **84**, (1977), 91-92.

Churchill, S.W., and Chu, H.H.S.: Correlating equations for laminar and turbulent free convection from a horizontal cylinder, *International Journal of Heat and Mass Transfer*, **18**, (1975), 1049-1053.

Dai, C., Chen, Y., and Zhao, J.: An Experimental Simulation on Heat Transfer Characteristics of a Downhole Heat Exchanger, *Proceedings,* 34th Workshop on Geothermal Reservoir Engineering, Stanford University, Stanford, CA (2009).

Dai, C., Xie, S., Lei, H., Wang, Y., and Sun, P.: A case study of space heating using a downhole heat exchanger in China, *GRC Transactions*, **35**, (2011), 1077-1080

Davis, A.P., and Michaelides, E.E.: Geothermal power production from abandoned oil wells, *Energy*, **34**, (2009), 866-872.

Freeston, D.H., and Pan, H.: The application and design of downhole heat exchanger, *Geothermics*, **14(2)**, (1985), 343-351.

Fridleifsson, I.B.: Geothermal energy for the benefit of the people, *Renewable & Sustainable Energy Reviews*, **5**, (2001), 299-312.

Gnielinski, V.: New Equations for Heat and Mass Trans-fer in the Turbulent Flow in Pipes and Channels, *International Chemical Engineering*, **16**, (1976), 359-368.

Higgins, B.S., Oldenburg, C.M., Muir, M.P., Pan, L., and Eastman, A.D.: Process Modeling of a Closed-Loop SCO2 geothermal Power Cycle, *Proceedings,* 5th International Supercritical CO_2 Power Cycles Symposium, San Antonio, Texas (2016).

Jalaluddin, and Akio, M.: Thermal performance investigation of several types of vertical ground heat exchangers with different operation mode, *Applied Thermal Engineering*, **33-34**, (2012), 167-174.

Lund, J.W.: The use of downhole heat exchangers, *Geothermics*, **32**, (2003), 535-543.

Luo, J., Rohn, J., Bayer, M., and Priess, A.: Thermal performance and economic evaluation of double U-tube borehole heat exchanger with three different borehole diameters, *Energy and Buildings*, **67**, (2013), 217-224.

Riahi, A., Moncarz, P., Kolbe, W., and Damjanac, B.: Innovative Closed-Loop Geothermal Well Designs Using Water and Super Critical Carbon Dioxide as Working Fluids, *Proceedings,* 41st Workshop on Geothermal Reservoir Engineering, Stanford University, Stanford, CA (2017).

Shi, Y., Song, X., Li, G., Yang, R., Shen, Z., and Lyu, Z.: Numerical investigation on the reservoir heat production capacity of a downhole heat exchanger geothermal system, *Geothermics*, **72**, (2018), 163-169.

Song, X., Shi, Y., Li, G., Yang, R., Xu, Z., Zheng, R., Wang, G., and Lyu, Z.: Heat extraction performance simulation for various configurations of a downhole heat exchanger geothermal system, *Applied Thermal Engineering*, **141**, (2017), 1489-1503.

Song, X., Zheng, R., Li, G., Shi, Y., Wang, G., and Li, J.: Heat extraction performance of a downhole coaxial heat exchanger geothermal system by considering fluid flow in the reservoir, *Geothermics*, **76**, (2018), 190-200.

Tago, M., Morita, K., and Sugawara, M.: Heat extraction characteristics of a single U-tube downhole heat exchanger with square cross section, *International Journal of Heat and Mass Transfer*, **42**, (2006), 608-616.

Wang, J., Ren, C., Gao, Y., Chen, H., and Dong, J.: Performance investigation of a new geothermal combined cooling, heating and power system, *Energy Conversion and Management*, **208**, (2020), 112591.

Zeng, H., Diao, N., and Fang, Z.: Efficiency of vertical geothermal heat exchangers in the ground source heat pump system, *Journal of Thermal Science*, **12**, (2003), 77-81.

Zhang, Y., Yu, C., Li, G., Guo, X., Wang, G., Shi, Y., Peng, C., and Tan, Y.: Performance analysis of a downhole coaxial heat exchanger geothermal system with various working fluids, *Applied Thermal Engineering*, **163**, (2019), 114317.